Project Report
TIP-175

Lidar for High-Altitude, Long-Endurance (HALE) Environmental Monitoring: FY21 Technical Investment Program

W.D. Herzog
D.S. Wolinski
M.C. Stowe
C.A. Primmerman
J.B. Ashcom
J. Khan
T.Y. Fan
J.A. Dykema

18 May 2023

Lincoln Laboratory
MASSACHUSETTS INSTITUTE OF TECHNOLOGY
LEXINGTON, MASSACHUSETTS

This material is based upon work supported by the United States Air Force under Air Force Contract No. FA8702-15-D-0001.

This report is the result of studies performed at Lincoln Laboratory, a federally funded research and development center operated by Massachusetts Institute of Technology. This material is based upon work supported by the United States Air Force under Air Force Contract No. FA8702-15-D-0001. Any opinions, findings, conclusions or recommendations expressed in this material are those of the author(s) and do not necessarily reflect the views of the United States Air Force.

Massachusetts Institute of Technology
Lincoln Laboratory

Lidar for High-Altitude, Long-Endurance (HALE) Environmental Monitoring: FY21 Technical Investment Program

W.D. Herzog
Group 81

D.S. Wolinski
Group 97

M.C. Stowe
J. Khan
Group 6

C.A. Primmerman
Div 9

J.B. Ashcom
Group 91

T.Y. Fan
Group 82

J.A. Dykema
Harvard University

Project Report TIP-175

18 May 2023

This material is based upon work supported by the United States Air Force under Air Force Contract No. FA8702-15-D-0001.

Lexington Massachusetts

This page intentionally left blank.

ABSTRACT

Aerosols are both direct radiative forcing agents, scattering solar radiation back to space and absorbing solar and terrestrial radiation, and indirect radiative forcing agents, modifying the albedo of clouds. Tropospheric aerosols are thought to account for ~80% of aerosol radiative forcing, but the contribution from stratospheric aerosols is highly uncertain; the radiative forcing due to stratospheric aerosols is suggested to be uncertain by ±100%. This uncertainty stems from a poor understanding of the composition, and hence complex refractive index, of the aerosol. Improving our observation capabilities of stratospheric aerosols could help reduce their radiative forcing uncertainty. This study evaluated the feasibility of placing a bistatic lidar on a pair of high-altitude UAVs to retrieve the properties of the stratosphere's aerosol.

ACKNOWLEDGEMENTS

The authors would like to express their deep gratitude to John Dykema of Harvard University for all the contributions he made to our weekly discussions. His guidance on climate science was critical to our project.

TABLE OF CONTENTS

LIST OF FIGURES

1. INTRODUCTION

During the past year, staff at MIT Lincoln Laboratory (MIT LL) have begun to evaluate the feasibility and utility of an aerosol-sensing lidar on high-altitude, long-endurance (HALE) UAVs for improving our understanding of stratospheric aerosols. Aerosols affect the Earth's energy budget and atmospheric chemistry in several important ways. They directly impact the Earth's radiation balance by scattering and absorbing solar radiation, they indirectly affect the radiation balance through their roles in cloud formation and the water cycle, and they serve as a catalyst for chemical reactions in the upper atmosphere.

Aerosol radiative forcing currently has the largest uncertainty in the budget of anthropogenic perturbations to the climate's radiative balance [1]. Tropospheric aerosols likely cause significant direct and indirect radiative forcing. The magnitude of this forcing is thought to be equal in magnitude to the warming effect of greenhouse gases [1]. However, the uncertainty in the magnitude of the contribution of tropospheric aerosols to radiative forcing is also very large. For tropospheric aerosols, improved retrieval of the aerosol size distributions and their optical constants (real and imaginary index of refraction) are needed to better understand their direct radiative impact. Additionally, low-lying tropospheric aerosols, such as those over the Pacific Ocean, are critical to cloud formation, cloud depth, and water content.

Stratospheric aerosols are thought to have a smaller contribution to direct radiative forcing, likely accounting for ~20% of the total direct aerosol forcing [2]. However, even less is known about these aerosols. Until recently, stratospheric aerosols were assumed to be simple sulfuric acid/water solution droplets that episodically would be augmented by volcanically derived sulfur aerosols that increased the fraction of larger particles. More recently, airborne in-situ measurements have suggested that stratospheric aerosols may contain highly absorbing carbonaceous components [3]. It was recently suggested by our collaborator, John Dykema of Harvard University, that the uncertainty in the composition and refractive indices of stratospheric aerosols could cause a ±100% change in radiative forcing of the stratosphere [4]. Similar to the sensing needs for tropospheric aerosols, stratospheric science would benefit from better characterization of the aerosol composition and size distributions.

As anthropogenic emissions further modify the atmosphere, it is important that we establish a well-characterized baseline of the current (and historical) atmospheric state. Looking forward, if geo-engineering mitigations are realized, such as the introduction of aerosols into the stratosphere to increase direct radiative scattering, observation systems will be needed to study the distribution, evolution, and ancillary impacts of these aerosols on the stratosphere.

As part of this study, the MIT LL team developed an appreciation for a variety of aerosol-sensing missions. The MIT LL study generally focused on aerosol retrieval in the stratosphere. This is a very challenging mission due to the very small sizes and concentrations of the aerosol. As a baseline, we considered a bistatic lidar carried aboard a pair of HALE UAVs like those proposed to the MIT Climate Initiative by the Stratospheric Airborne Climate Observatory System (SACOS) to Initiate a Climate Risk Forecasting Revolution team. These HALE UAVs are to be solar-powered aircraft that loiter for long periods of time at altitudes between 14 km and 20 km. Although each SACOS UAV is tailored to specific climate-sensing missions, they typically have wingspans of ~40 m, can carry payloads of ~30–50 kg and provide the scientific payload with ~500 W during daylight hours and ~150 W at night.

During the study, the team identified three possible missions for remote stratospheric aerosol monitoring. The easiest mission would be to map the injection of tropospheric materials into the stratosphere, which alters the local atmospheric chemistry. This mission doesn't require aerosol retrieval, per se, as the regions of tropospheric injection exhibit very large aerosol scattering relative to the rest of the stratosphere, making them easy to map. The next level of difficulty would be to deploy a lidar system capable of retrieving the bimodal aerosol distribution, quantifying the fraction of coarse and fine modes. This would provide spatial distributions to what are currently global averages of quiescent and volcanic-influenced stratospheric size distributions. Finally, the ideal system would be able to measure the complex refractive indices and ratios of the bimodal distribution of stratospheric aerosol.

2. STUDY OVERVIEW

The aerosol lidar study at MIT LL has primarily considered three aspects of an airborne aerosol lidar. First, the team developed a simulation tool to understand the aerosol retrieval accuracy for a variety of system geometries and configurations. This tool is critical to understanding how to optimally design and build a measurement system to retrieve the aerosol properties with the necessary accuracy. Second, we leveraged existing atmospheric optical and lidar modeling tools used at MIT LL, Betaspec [5], and MODTRAN [6] to estimate the lidar link budget or signal-to-noise ratio (SNR). These models, which include aerosol and Rayleigh scattering, solar background, and atmospheric attenuation, enable us to understand how high-level requirements flow down to the requirements of the lidar components. Finally, through building the models and comparing the system requirements with traditional laser detection and ranging (LADAR) systems that we have designed, the team has started to identify the unique challenges and risks associated with a multi-platform observation system. We have also begun to consider how emerging state-of-the-art technologies that we currently are working on might address the challenges of a HALE UAV aerosol lidar.

To improve aerosol retrieval, one needs a system that is capable of providing multiple independent measurements of the aerosol. Existing monostatic high spectral resolution lidars (HSRLs), such as NASA's CALIOP [7], typically provide at most five independent measurements that provide insufficient information to solve for the unknown parameters describing a bimodal aerosol distribution with unknown optical constants for the constituent materials. To overcome this deficiency, the MIT LL team pursued the approach proposed in 2016 by Michael Mishchenko, a world renowned radiative-transfer theorist and senior scientist at NASA. Mishchenko advocated for a bi-static observation system to increase the number of observations and improve aerosol retrieval [8].

Our study extended the work on Mishchenko et al. to evaluate possible system configurations on HALE UAVs for aerosol retrieval. For stratospheric aerosols, the lidar system would primarily be looking up, whereas for tropospheric aerosols and for the cubesats considered by Mishchenko and collaborators, the systems are looking downward. The basic geometry considered is shown in Figure 1.

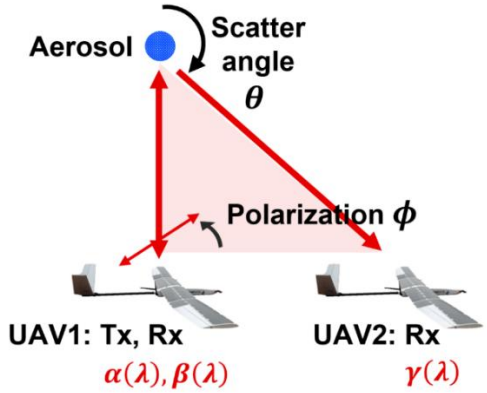

Figure 1. Geometry of a bi-static HALE UVA aerosol lidar. The first UAV has both a polarization-controlled transmitter and a receiver to measure backscattered light, and the second UAV has only a polarized receiver. The system operates at one or more wavelengths.

This page intentionally left blank.

3. AEROSOL RETRIEVAL MODEL

The MIT LL team developed a system-analysis tool for simulating the retrieval of atmospheric aerosol parameters using a high spectral resolution lidar (HSRL) system. Figure 2 shows a block diagram of the tool, comprised of a forward model that simulates noisy measurements of a target aerosol, and an inference engine that estimates aerosol parameters from those measurements. The tool provides two important capabilities. First, we can optimize the conceptual design of an HSRL system intended for measuring different aerosols subject to system constraints such as the available measurement modalities and SNR. Second, for a particular HSRL system, we can estimate the correlated retrieval errors and their dependence on system parameters.

The forward model simulates the optical measurements of a particular aerosol made by an HSRL system with a particular configuration. The system configuration defines the transmitter/receiver geometry (e.g., bistatic angles), the transmitted laser wavelengths (e.g., 355 nm, 532 nm, 1064 nm) and polarization states (e.g., linear), and the measured spectral channels and polarizations (e.g., linear, circular). The total aerosol is modeled as a set of individual populations of homogeneous spheres. Each population is described by a set of aerosol parameters (to be retrieved) defining a monomodal size distribution, complex index of refraction, and atmospheric concentration. The Mie scattering from the total aerosol population is calculated in each receiver direction to yield optical measurements consisting of the spectrally resolved quantities of extinction, backscatter irradiance, and multiple side-scatter polarimetric irradiances (from the outputs of different optical analyzers). We assume independent Gaussian measurement errors given by simple SNR considerations (typically ~10%), which will be refined by the lidar system model link budget analysis.

The inference engine solves the inverse problem of retrieving the unknown aerosol parameters from a set of noisy measurements made by an HSRL system. First the forward-model function is linearized in the neighborhood of a solution guess. We then form a maximum-likelihood estimate of the aerosol parameters using a Bayesian technique with uniform priors modified from [9]. Potential bias errors in the retrieved parameters arising from the linear approximation are greatly reduced by repeating incremental retrievals until convergence, at the cost of additional compute time.

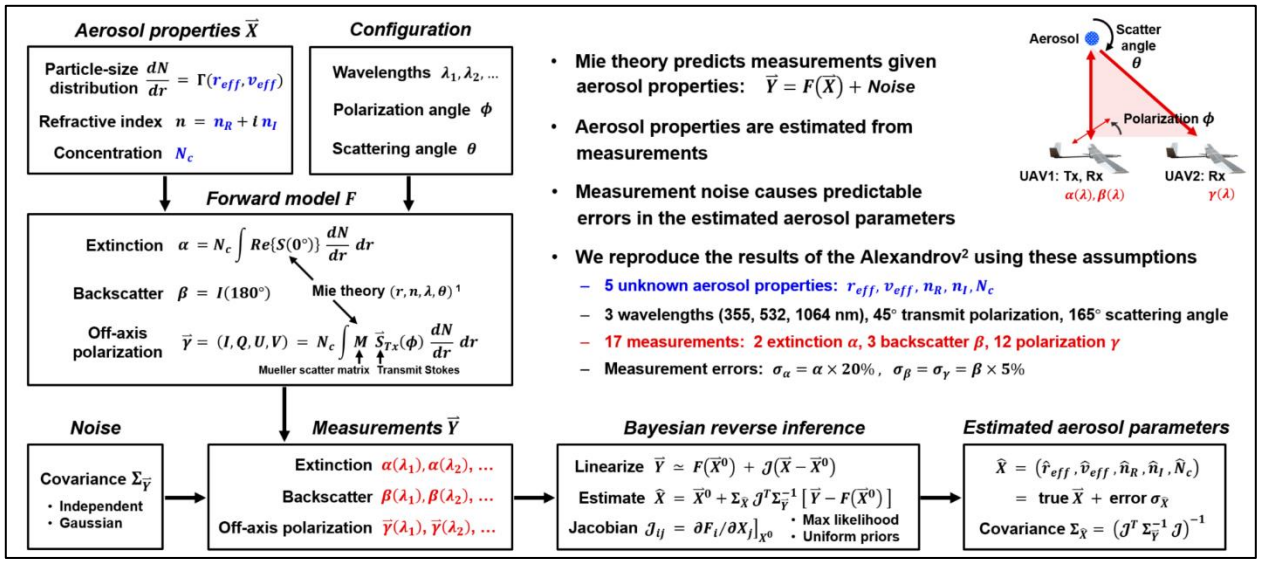

Figure 2. System-analysis tool developed to estimate aerosol retrieval performance for a variety of system configurations and geometries. The text highlights retrieval of a single aerosol distribution (5 parameters) using a bi-static, three-color, polarimetric, and lidar (17 measurements) to compare with the results of Mishchenko and Alexandrov.

The system-analysis tool has been validated against published results [10] for the case of a simulated bistatic HSRL providing 17 total measurements over three wavelengths ("12γ + 3β + 2α" configuration) against monomodal aerosols. We have also studied retrieval performance against bimodal stratospheric aerosols specified by Deshler [11, 12]. Table 1 lists the inputs used to evaluate the ability of a two-color HSRL polarimetric lidar to retrieve a stratospheric bimodal aerosol, which is a more challenging retrieval because we are attempting to estimate more unknown aerosol parameters (9) using fewer measurements (12). Figure 1 shows the relative precision (statistical error due to measurement noise) vs. scattering angle for each retrieved aerosol parameter. Although the angular dependence of each estimated parameter is unique, this result is useful for identifying a common angle that yields near-optimal estimation of all parameters (in this case, about 130°). Similar analyses were performed to optimize other HSRL parameters to achieve best performance (e.g., transmit polarization at 45°).

TABLE 1
Model Inputs to Evaluate the Ability of a Two-Color HSRL Polarimetric Lidar to Retrieve a Stratospheric Bimodal Aerosol of Deshler

			Forward model truth			Mismatch error
			Mode 1	Mode 2		Difference between assumptions made during inference and truth
Aerosol properties	Lognormal PSD	CMD (nm)	80	400		None
		GSD	1.6	1.15		None
	Real index n_R		1.45	1.45		None
	Imag index n_I (not estimated)		0.003			None
	Total concentration N_c (cm^{-3})		1000			None
	Coarse mode fraction CMF		0.01			None
Configuration	Wavelengths λ		266, 532 nm			None
	Polarization angle ϕ		45°			None
	Scattering angle θ		Vary from 0 - 180°			None
Observations	12 measurements		2 extinction α	2 backscatter β	8 polarization γ	
	Statistical error (independent)		$\alpha \times 10\%$	$\beta \times 10\%$	$\gamma \times 10\%$	

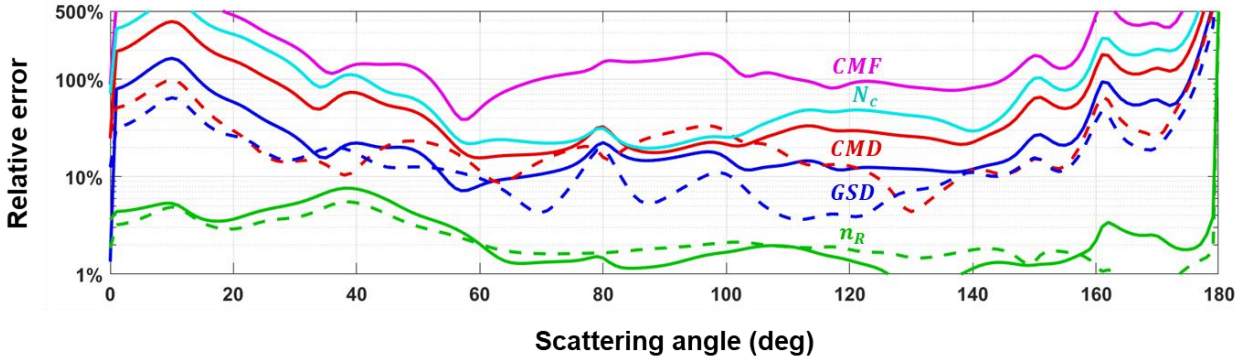

Figure 3. Relative error vs. scattering angle for retrieved aerosol parameters: number concentration (NC), coarse mode fraction (CMF), count median diameter (CMD), geometric standard deviation (GSD), and real index of refraction (nR), for the coarse (dashed) and fine (solid) populations of a bimodal aerosol of Deshler.

We have also used the system-analysis tool to estimate the accuracy (systematic error due to mismatch between model and truth) of the retrieved aerosol parameters. This allows us to understand both the cause and magnitude of potential estimation biases due to the retrieval process itself, as opposed to the statistical errors rooted in measurement noise as discussed above. The linear approximation used during inference is one example cause of bias error. Figure 2 shows the relative bias of the retrieved fine-mode aerosol parameters as a function of the mismatch between the true and assumed values of two particular aerosol parameters, GSD and real index. As mismatch increases, each parameter estimate acquires a bias according to the strength of its nonlinear influence on the measurements. Understanding the cause of an important systematic error can then inspire possible mitigations: initial results of an iterative estimation method, a modification to the retrieval process, suggest that this bias can be significantly reduced. We have also studied the estimation bias due to the mismatch of other system parameters such as scattering and polarization angles in a similar way. Finally, we are beginning to use the tool to understand the information

tradeoff among the many possible configurations of a system design (particularly the analyzed polarization states).

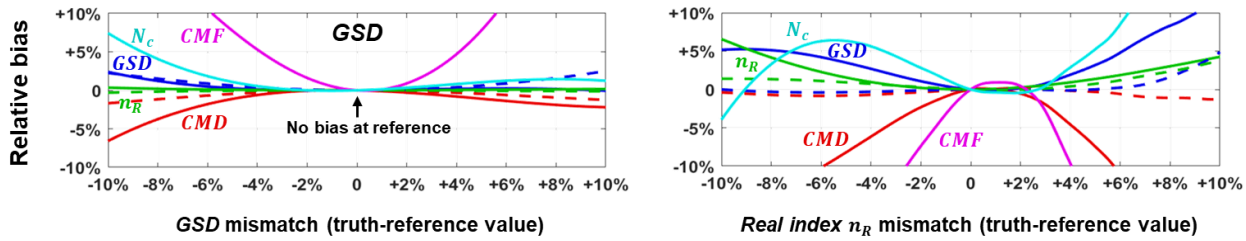

Figure 4. Relative bias of the retrieved fine-mode aerosol parameters vs. the difference between the true and assumed values of aerosol parameters GSD (left) and real index (right).

4. LIDAR LINK BUDGET MODELING

Although the MIT LL team has extensive experience developing aerosol point sensors [13] and airborne 3D LADAR imaging systems [14], the Laboratory staff do not have experience designing aerosol lidars. The team leveraged common modeling tools in use at the MIT LL, BetaSpec and MODTRAN, and began by validating our modeling results to a well-documented aerosol lidar, the NASA CALIOP system [15] and checking the aerosol scattering coefficients in BetaSpec against the calculated cross-sections of in-situ balloon-based measurements [16]. Having validated the aerosol terms in BetaSpec and our model vs. published CALIOP results, we have begun to model a bistatic aerosol lidar.

Balloon-borne particle measurements are seen in Figure 5a. For this project, we averaged across all the balloon sounding events to arrive at a time-averaged aerosol column. Using the aerosol sizing data and Mie scattering theory, we converted the measurements into scattering coefficients versus altitude (Figure 5b). Figure 6 shows the comparison of the balloon-borne scattering coefficients vs. that default atmosphere in BetaSpec. We found good agreement between the altitude dependence of these two sources and proceeded to use the BetaSpec atmosphere.

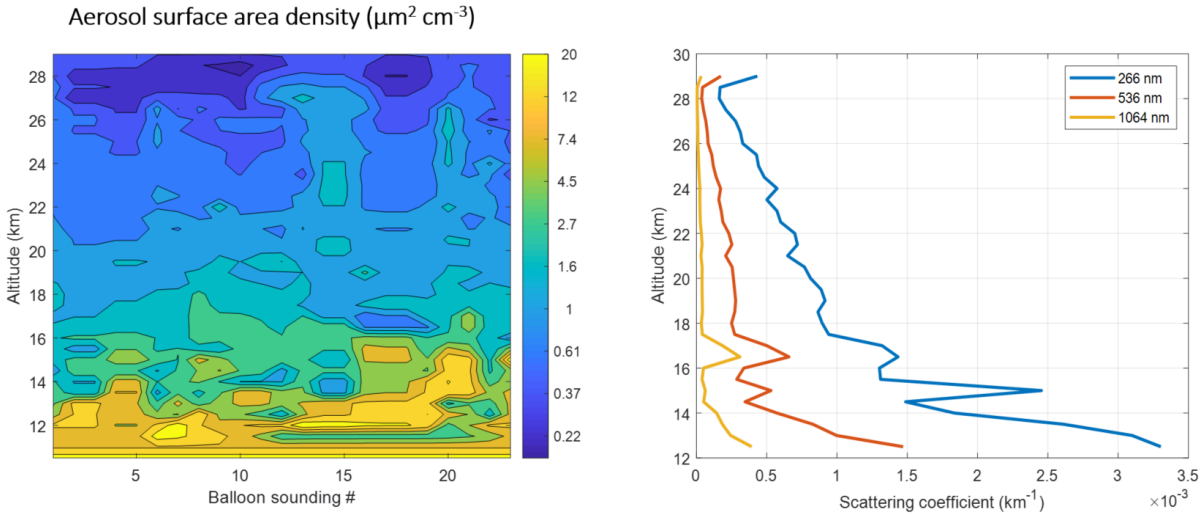

(a) (b)

Figure 5. Balloon particle counter data (left) and calculated scattering coefficients for three laser wavelengths vs. altitude (right).

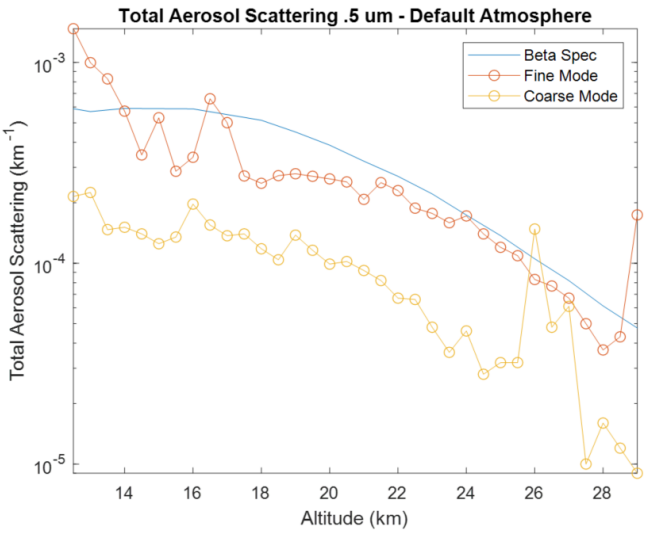

Figure 6. Aerosol scattering coefficients derived from balloon-borne data compared to the default atmosphere of BetaSpec.

Figure 7 depicts the configuration of the bistatic system and Figure 8 shows the anticipated signal levels from the bistatic lidar model for the monostatic system. For this model, we assumed that the lidar transmitter had a 10-cm diameter aperture and each lidar carried a 10-cm diameter receive aperture. The laser is transmitted 45° relative to zenith with an assumed power of 10 W and pulse rate of 20 Hz at all four 1064 nm harmonics (1064 nm, 532 nm, 355 nm, and 266 nm). Note that the pulse duration need only be less than the desired range resolution of 250 m or 1.6 µs, an easily achieved constraint. The lidar receivers are assumed to have a 30% efficient optical transmission, 0.4 nm optical passband, and a 10% quantum efficiency. The receiver on platform 2 is assumed to be a 32-channel PMT detector for range resolution along the transmitted beam.

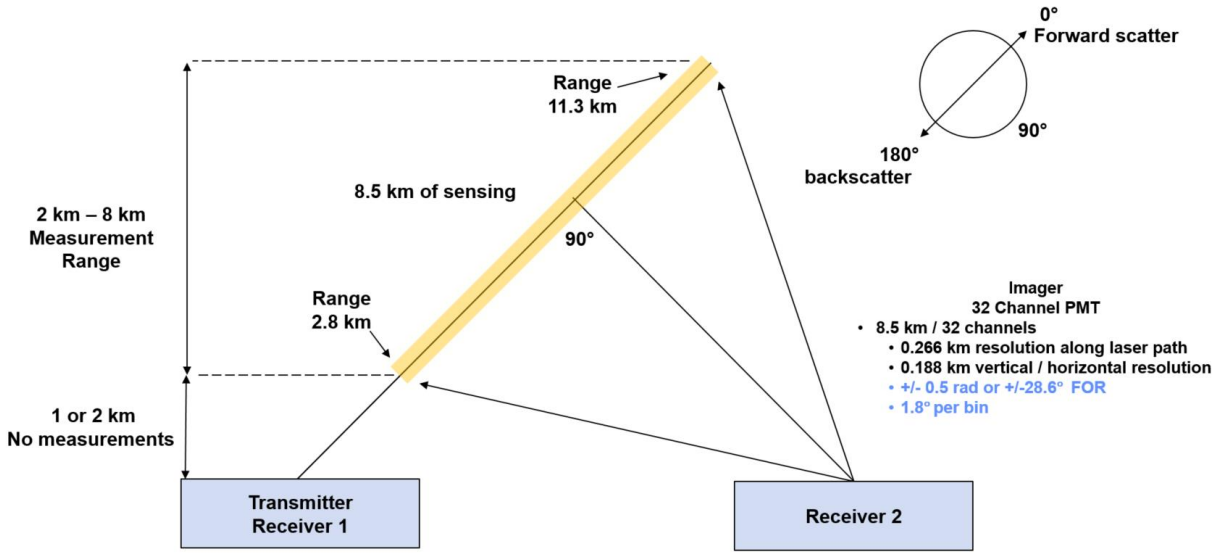

Figure 7. Configuration of the two UAV platforms used for the lidar model.

The bistatic link calculation was conducted for both UAV platforms at an altitude of 18 km looking up into the stratosphere at 45° zenith. As can be seen in Figure 6, platform 1 is the transmitter (with a monostatic receiver) and platform 2 is a dedicated to detecting the light scattered from the pulsed transmitted laser beam. To enable range resolution along the transmitter, path the bistatic receiver has a 32-channel PMT with each channel looking at a different angle and thus range bin along the transmitter. Our climate science collaborator in this study, John Dykema, informed us that 32 range bins of about 266 m length would be a relevant spatial sampling. Due to the fact that the UAVs are solar powered, we included solar downwelling radiance via MODTRAN. Solar is the dominant noise source for platform 2 due to the required field-of-view (FOV) of each PMT channel. We considered the FOV for each detector in the array to be independently adjustable. One dimension is fixed by the desired range resolution, and the other, orthogonal dimension of the FOV or cross range is a design parameter. For the bistatic results presented below, the cross range was chosen to be 10 m. This places a burden on the relative pointing accuracy between platforms while also reducing the solar noise sufficiently to obtain a reasonable SNR rate.

Figure 8 depicts the molecular scattering signal (Rayleigh) and the aerosol signal for the monostatic system. As is typical of aerosol lidars, the molecular scatter is comparable to or larger than the aerosol scattered signal. In fact, in the stratosphere, the molecular scattering dominates the aerosol scatter as can be seen in the left-hand panel of Figure 8. High spectral resolution techniques have been developed to filter out the narrowband (MHz) aerosol signal, allowing a direct measurement of the order GHz bandwidth molecular scatter signal. This direct molecular scattering signal can then be used to estimate and remove the molecular background signal and thus estimate the aerosol signal level.

We define the SNR as aerosol counts to square root of total counts. Note that the actual measured signal level is the total counts from aerosol scatter, molecular scatter, and solar. So, although the measurement is expected to be shot noise limited, it is not signal shot noise limited. The assumption is that the solar and molecular contributions can be estimated and removed to recover the aerosol-only signal, but the noise due to molecular and solar cannot be removed without very (<GHz) narrowband optical filtering. For the monostatic lidar on platform 1, the solar contribution is very low due to the narrow FOV, but quite significant on platform 2.

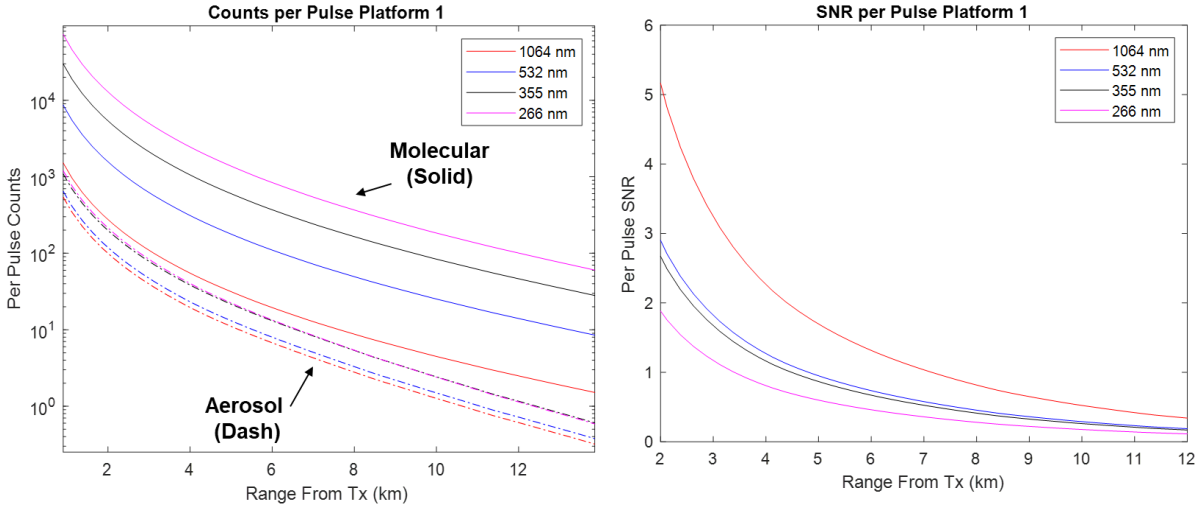

Figure 8. (Left) Rayleigh (molecular) solid line and aerosol backscattering signals dashed lines in photo electrons per pulse vs. range for the monostatic receiver; (right) per pulse SNR.

Figure 9 shows the ratio of the signal from the molecular backscatter to the aerosol backscatter expected for the monostatic lidar on platform 1. This ratio demonstrates a key challenge for atmospheric aerosol lidars in that the signal offset due to the molecular scatter must be estimated and removed to enable accurate aerosol backscatter levels or to estimate the number density of a known cross-section aerosol.

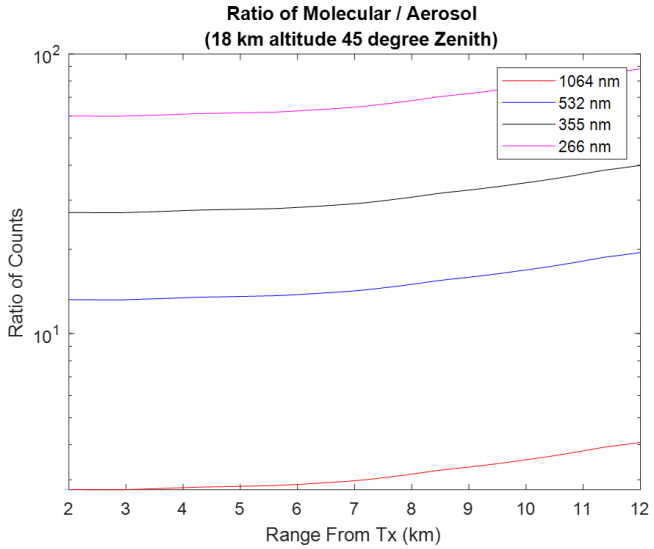

Figure 9. Ratio of molecular to aerosol signal levels.

We now address the link for the bistatic platform, platform 2. Unlike the monostatic receiver, the receiver of platform 2 will be polarimetric and measure the angular dependence of the scattering due to the variation of line-of-sight angle vs. range along the transmitted beam shown in Figure 7. To estimate the scattering phase function for the molecular P-polarized light, we use a $\cos^2$ dependence and no angular dependence for S-polarized scatter. The specific aerosol properties must be assumed to estimate an example design point link; in practice, the goal is to measure these properties. For this, the Deshler model was used with Mie scattering code to estimate the phase function for both S- and P-polarizations. This polarization-dependent phase function was then used to scale the BetaSpec volume backscatter values vs. scattering angle. One of the advantages of the bistatic configuration is that the P-polarized light scattered from the molecules is suppressed at 90°, illustrated in Figure 10, left panel. This allows a lower noise, more direct measurement of the aerosol contribution. In contrast, the S-polarization does not exhibit this molecular scatter suppression (see Figure 10, right panel).

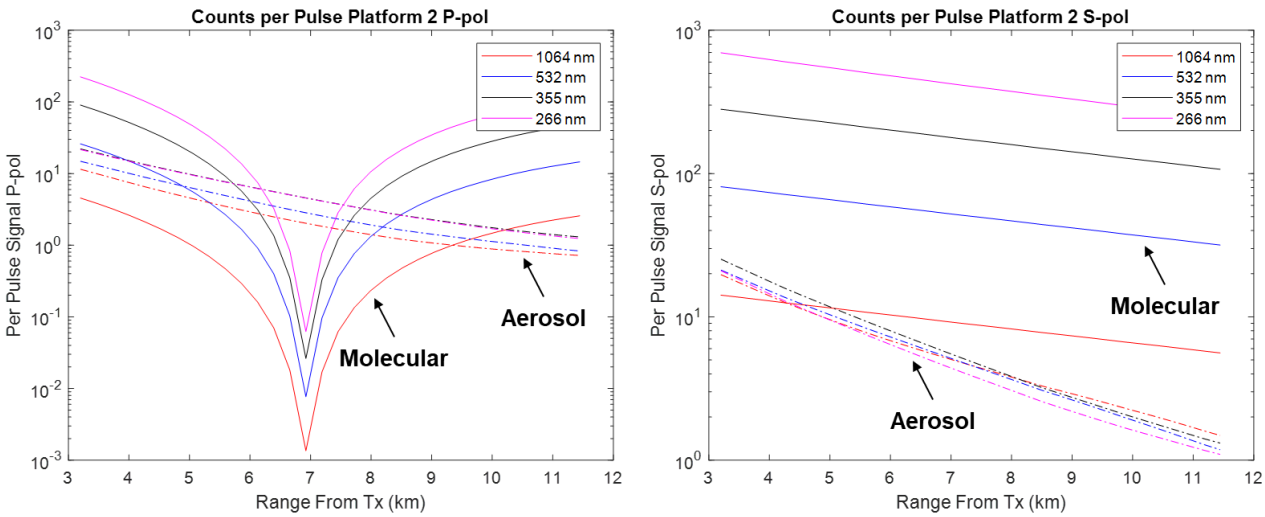

Figure 10. (Left) Per pulse P-polarized signal counts vs. range along the transmitter vs. wavelength and scattering type. Note molecular scatter suppression at 90° for P-polarization; (right) same, but for S-polarized.

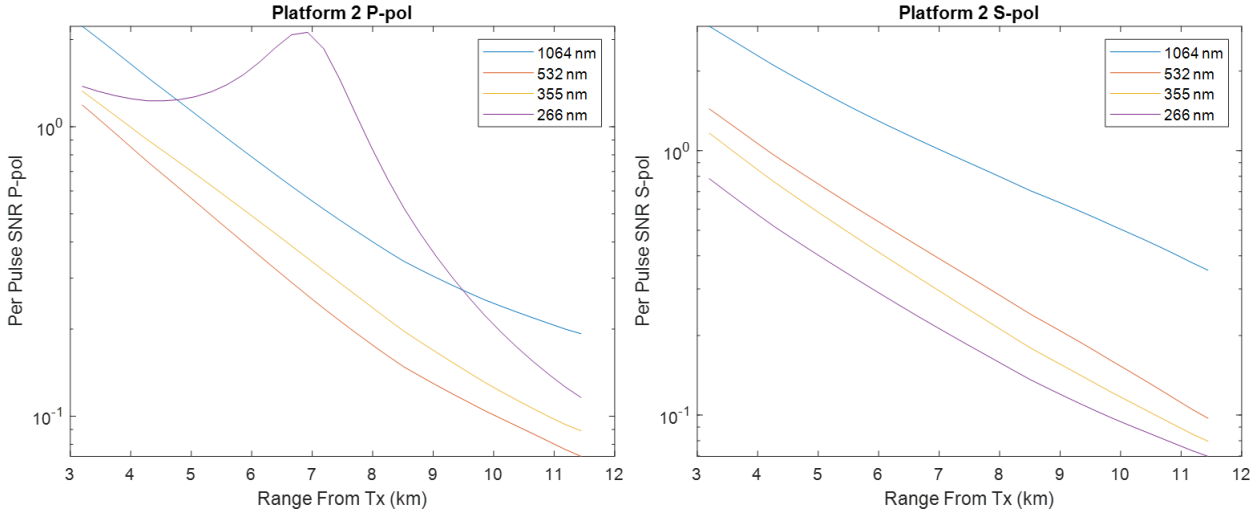

Figure 11. Platform 2 per pulse SNR vs. range and polarization.

Finally, in Figure 11, the resulting per-pulse SNR for the bistatic configuration is shown. The large increase in the 266 nm SNR results from the molecular suppression and the fact that MODTRAN has identically zero solar radiance at 266 nm. The noise for all other wavelengths is dominated by solar contributions due to the large FOV required on platform 2. Results from this type of system-link analysis can be coupled with the aerosol parameter estimation model presented in the previous section to determine a required SNR and thus number of pulses and averaging time.

This page intentionally left blank.

5. LIDAR SYSTEM CHALLENGES AND OPPORTUNITIES

Development of a bistatic lidar for studying stratospheric aerosols presents several design challenges. The two major challenges are the low signal levels and the large number of aerosol parameters that one is attempting to retrieve via the remote measurements. Additional challenges include the coordination of the pointing between the two aircraft; the wide FOV of the laser path viewed from platform 2 that results in a large solar background flux and the fact that the transmitted laser does not have a beam stop, such as the surface of the Earth for downward looking lidars.

The low signal levels associated with stratospheric aerosols limit one's ability to collect high SNR data from the SWAP-constrained HALE-UAVs, as evidenced in Figures 8 and 11. This challenge of a limited SNR per measurement is amplified by the fact that the bistatic lidar system needs to make multiple, independent measurements by varying the scattering angle, polarization, and wavelength to retrieve the 10 parameters that are needed to describe the bimodal aerosol distribution. Further constraining the problem is the desire to maintain a spatial resolution that captures the structure expected within the stratospheric layers; ~2 km vertical spatial features and ~150 km horizontal spatial features.

Although the study did not reach a definite conclusion as to whether a bistatic lidar on solar powered HALE UAVs could retrieve all the parameters of a bimodal stratospheric aerosol distribution, the team did develop alternative mission and sensor concepts that were less ambitious as a risk mitigation. One mission that was identified for a HALE UAV lidar was wide-area mapping of tropospheric aerosol injection into the stratosphere. Wildfires, thunderstorm deep convection, and volcanic events have all been observed to inject larger aerosols into the stratosphere. Mapping the spatial extent and evolution of injected material would provide scientific value and be less demanding on a lidar system, as the injection events would be evident from the increase in scattering cross section of the tropospheric material.

Alternatively, it would be much easier to build an optical, single-particle point sensor that fully characterized the bimodal stratospheric aerosol distribution than to do it remotely with a lidar. For the case of a point sensor, one has considerable advantages in terms of signal and SNR per measurement. In addition, the challenge of retrieving 10 parameters that describe the aerosol distribution collapse into the measurement of 3 parameters per particle in the single-particle case. For single particle measurements, one needs to measure the size of each particle and its complex index of refraction (real and imaginary part). This is done for particles comprising both modes of the size distribution. The remaining parameters, the mean sizes for each mode, their standard deviation, and its total mass, or concentration, is determined through repeated single-particle measurements and the statistics collected over the ensemble of measurements.

Another challenge the team identified is that the two platforms need to coordinate their FOVs as the two aircraft pitch, roll, and yaw. There are a couple challenges this presents. First, pointing control is typically done with closed-loop active pointing systems, or gimbals. However, gimbals can be very large and consume a lot of power. For our bistatic lidar system, special attention will need to be paid to this component and we've begun to identify some options. A second challenge presented by the platform-to-platform motion is the non-idealities this introduces into the polarimetery. As the transmit aircraft yaws, the axis of polarization rotates with the aircraft. Fortunately, the aerosol retrieval model we have built can help us understand the impact of this motion.

Another unique aspect is the bimodal receiver, its orientation and FOV. Because of the wide FOV along the laser path, a vapor cell would probably need to be used to narrow the spectral response bandwidth in lieu of etalons. One technology we are considering for this is a new wide FOV filter MIT LL recently patented and developed for trace vapor sensing. This technology could a two-port observation system that allows better extraction of the aerosol signal from the molecular Rayleigh scattering.

Called NIFTy (Narrowband Imaging Filter Technology, US Patent 10,794,819), the system is based on imaging through a two-path interferometer where one arm has a gas cell containing the specific gas to be detected. The small change in the index of refraction at each absorption line unbalances the interferometer at only those wavelengths, creating a filter with passbands exactly matched to the target gas, enabling detection and quantification. Because the filter exhibits high out-of-band rejection, and because the passbands are matched in width to the ~ 1 GHz-wide air-broadened absorption lines of the target, passive radiation (from solar reflection or ground emission) is used optimally for the highest SNR. The creation of multiple passbands at many individual absorption lines within a vibrational band yields high specificity. The combination of high spectral resolution and wide FOV, supporting an imaging mode and high area coverage rate, cannot be obtained with traditional imaging spectrometers or FTIRs. The high spectral resolution also enables access to regions of the atmosphere with significant water or CO_2 absorption, because it is possible to identify target absorption lines between these interferent lines that would be integrated over and obscured by lower-spectral resolution instruments.

Finally, the bimodal receiver geometry also offers a unique advantage relative to monostatic aerosol lidars; the ability to position platform 2 exactly in the null of the molecular scattering. As shown in Figure 7, platform 2 can be positioned at 90° relative to the laser propagation direction. For this scattering angle in the P-polarized scattering geometry, the molecular scattering is two to three orders of magnitude weaker than for other scattering angles. This offers the possibility of positioning the platform where the aerosol scattering would dominate that from the molecular contribution. One could imagine scanning the transmitted laser beam such that, for each spatial slice in altitude, platform 2 is positioned in the null of the molecular scattering for the measurement. This strategy would significantly help with the low SNR, but constrains the lidar in the number of independent observations it makes.

In summary, during the past year, staff at MIT LL have begun to evaluate the feasibility and utility of an aerosol-sensing lidar on HALE UAVs for improving our understanding of stratospheric aerosols. The team developed a simulation tool to understand the aerosol retrieval accuracy for a variety of system geometries and configurations. This tool is critical to understanding how to optimally build a measurement system to retrieve the aerosol properties with the necessary accuracy. Second, the team leveraged existing atmospheric optical and lidar modeling tools used at MIT LL to estimate the lidar link budget or SNR. These models, which include aerosol and Rayleigh scattering, solar background, and atmospheric attenuation, enable us to understand how high-level requirements flow down to the requirements of the lidar components. Finally, through building the models and comparing the system requirements with traditional LADAR systems we have designed, the team has started to identify the unique challenges and risks associated with a multi-platform observation system.

6. REFERENCES

1. Stocker, T.F., et al., 2013: Technical Summary. In: Climate Change 2013: The Physical Science Basis. Contribution of Working Group I to the Fifth Assessment Report of the Intergovernmental Panel on Climate Change [Stocker, T.F., D. Qin, G.-K. Plattner, M. Tignor, S.K. Allen, J. Boschung, A. Nauels, Y. Xia, V. Bex and P.M. Midgley (eds.)]. Cambridge University Press, Cambridge, United Kingdom and New York, NY, US

2. Yu, P., Murphy, D. M., Portmann, R. W., Toon, O. B., Froyd, K. D., Rollins, A. W., et al. (2016). Radiative forcing 426 from anthropogenic sulfur and organic emissions reaching the stratosphere. Geophysical Research Letters, 427 43(17), 9361-9367.

3. Martinsson, Bengt G., et al. "Formation and composition of the UTLS aerosol." npj Climate and Atmospheric Science 2.1 (2019): 1-6.

4. Dykema, John A., Yaowei Li, and Frank N. Keutsch. "Composition dependence of stratospheric aerosol radiative forcing." AGU Fall Meeting Abstracts. Vol. 2020. 2020.

5. http://www.cas.usf.edu/lidarlab/betaspec.html

6. Berk, Alexander, et al. "MODTRAN® 6: A major upgrade of the MODTRAN® radiative transfer code." 2014 6th Workshop on Hyperspectral Image and Signal Processing: Evolution in Remote Sensing (WHISPERS). IEEE, 2014.

7. Winker, David M., William H. Hunt, and Chris A. Hostetler. "Status and performance of the CALIOP lidar." Laser Radar Techniques for Atmospheric Sensing. Vol. 5575. International Society for Optics and Photonics, 2004.

8. Mishchenko, Michael I., et al. "Multistatic aerosol–cloud lidar in space: A theoretical perspective." Journal of Quantitative Spectroscopy and Radiative Transfer 184 (2016): 180-192.

9. C.D. Rogers, Inverse Methods for Atmospheric Sounding: Theory and Practice (World Scientific, 2000).

10. M.D. Alexandrov and M. I. Mishchenko, "Information content of bistatic lidar observations of aerosols from space," Opt. Express 25, A134-A150 (2017).

11. Deshler, T., et al., "Thirty years of in situ stratospheric aerosol size distribution measurements from Laramie, Wyoming (41° N), using balloon-borne instruments," J. Geophys. Res., 108(D5), 4167, 2003.

12. Deshler, T., "A review of global stratospheric aerosol: Measurement, importance, life cycle, and local stratospheric aerosol," Atmos. Res., 90, 223-232, 2008.

13. Jeys, Thomas H., et al. Advanced trigger development. Massachusetts Institute of Technology-Lincoln Laboratory Lexington United States, 2007.

14. Albota, Marius A., et al. The airborne optical systems testbed (AOSTB). MIT Lincoln Laboratory Lexington United States, 2017.

15. Winker, David M., William H. Hunt, and Chris A. Hostetler. "Status and performance of the CALIOP lidar." Laser Radar Techniques for Atmospheric Sensing. Vol. 5575. International Society for Optics and Photonics, 2004.

16. The balloon data can be found on the Wyoming in situ data website http://www.atmos.uwyo.edu/~deshler/Data/Aer_Meas_Wy_read_me.htm

REPORT DOCUMENTATION PAGE

Form Approved
OMB No. 0704-0188

1. REPORT DATE *(DD-MM-YYYY)*	**2. REPORT TYPE**	**3. DATES COVERED** *(From - To)*
18/05/2023	Project Report	

4. TITLE AND SUBTITLE

Lidar for High-Altitude, Long-Endurance (HALE) Environmental Monitoring: FY21 Technical Investment Program

5a. CONTRACT NUMBER

5b. GRANT NUMBER

5c. PROGRAM ELEMENT NUMBER

6. AUTHOR(S)
W.D. Herzog, D.S. Wolinski, M.C. Stowe, C.A. Primmerman, J.B. Ashcom, J. Khan, T.Y. Fan, J.A. Dykema

5d. PROJECT NUMBER
TI04-03

5e. TASK NUMBER

5f. WORK UNIT NUMBER

7. PERFORMING ORGANIZATION NAME(S) AND ADDRESS(ES)

MIT Lincoln Laboratory
244 Wood Street
Lexington, MA 02421-6426

8. PERFORMING ORGANIZATION REPORT NUMBER

TIP-175

9. SPONSORING / MONITORING AGENCY NAME(S) AND ADDRESS(ES)

MIT LL Technology Office /Lab funded

10. SPONSOR/MONITOR'S ACRONYM(S)
MIT LL

11. SPONSOR/MONITOR'S REPORT NUMBER(S)

12. DISTRIBUTION / AVAILABILITY STATEMENT
DISTRIBUTION STATEMENT A. Approved for public release. Distribution is unlimited.

13. SUPPLEMENTARY NOTES

13. ABSTRACT

Aerosols are both direct radiative forcing agents, scattering solar radiation back to space and absorbing solar and terrestrial radiation, and indirect radiative forcing agents, modifying the albedo of clouds. Tropospheric aerosols are thought to account for ~80% of aerosol radiative forcing, but the contribution from stratospheric aerosols is highly uncertain; the radiative forcing due to stratospheric aerosols is suggested to be uncertain by ±100%. This uncertainty stems from a poor understanding of the composition, and hence complex refractive index, of the aerosol. Improving our observation capabilities of stratospheric aerosols could help reduce their radiative forcing uncertainty. This study evaluated the feasibility of placing a bistatic lidar on a pair of high-altitude UAVs to retrieve the properties of the stratosphere's aerosol.

15. SUBJECT TERMS

16. SECURITY CLASSIFICATION OF:			**17. LIMITATION OF ABSTRACT**	**18. NUMBER OF PAGES**	**19a. NAME OF RESPONSIBLE PERSON**
a. REPORT	**b. ABSTRACT**	**c. THIS PAGE**	None	26	**19b. TELEPHONE NUMBER** *(include area code)*
UNCLASSIFIED	UNCLASSIFIED	UNCLASSIFIED			